NANO LETTERS

2004
Vol. 4, No. 2
377−381

Gas Transport Characteristics through a Carbon Nanotubule

Sarah M. Cooper, Brett A. Cruden,*,† and M. Meyyappan

NASA Ames Research Center, Center for Nanotechnology, Moffett Field, California 94035

Reni Raju and Subrata Roy

Computational Plasma Dynamics Laboratory, Department of Mechanical Engineering, Kettering University, Flint, Michigan 48504

Received November 21, 2003; Revised Manuscript Received December 4, 2003

ABSTRACT

We report the first determination of the slip coefficient for tubular carbon structures that have been produced by chemical vapor deposition on a porous alumina substrate with nominal pore diameters of 200 nm. A uniform 20–30 nm thick carbonaceous coating was formed over the pores. The permeability of the porous alumina was then measured using a pressure/flow apparatus. A finite element code with adjustable slip boundary conditions was used to model transport through the alumina. In the absence of a carbonaceous material, transport was well described by diffuse reflection at the wall. When a carbon nanotubule was present, however, a tangential-momentum accommodation coefficient, σ_v, of 0.52 ± 0.1 was predicted for argon, nitrogen, and oxygen.

In a recent study, we reported measurements of diffusion rates through anodized alumina with 200 nm diameter pores and also demonstrated the applicability of a hydrodynamic model to capture the transport behavior within the pore.[1] The experimental data were consistent with the theoretical prediction, given the uncertainty in porosity. In the model employed, a first-order slip boundary condition was used, and a tangential-momentum accommodation coefficient (TMAC) of $\sigma_v = 1$ was found to successfully characterize transport through the pore, indicating that gas−wall interactions are described by diffusive reflection. Despite the theoretical elegance of molecular dynamics (MD),[2] direct simulation Monte Carlo (DSMC)[3] and Burnett equation[4] type models, they are yet to become applicable for practical micro/nano flow simulation. Although our finite element hydrodynamic model was successfully applied to microchannels and nanopores, it is expected that the standard hydrodynamic model assumptions will run into difficulties as the media for transport reach nanometer sizes. Among other things, the surfaces of the transport media should play a more prominent role in determining flow characteristics. In such a case, the flow properties could be significantly altered by controlling the nature of the pore surfaces. In this work, we have modified the alumina substrates with a carbonaceous coating and characterized gas transport through the tubule experimentally and theoretically. The combined approach has allowed for the determination of an effective TMAC for transport through the carbon nanotubules.

Fabrication of ordered pores on nanometer scales by aluminum anodization has been demonstrated by several groups over the past couple of decades.[5−7] Recently, renewed interest in these materials has arisen as a template material for nanotube growth,[8−11] electronic/magnetic/optical devices,[12,13] separations/filtration,[14,15] and energy storage.[16] For some of these applications, being able to understand and model flow characteristics through such media will become critical to their development. These porous media have been uniformly coated with different materials of varying thickness, including carbon and various metals.[8−11,16] Electrochemical transport through carbonaceous tubes prepared in this fashion has been studied by Miller et al.[15]

To produce the carbon nanotubules, we have employed a chemical vapor deposition (CVD) approach similar to that described in the literature.[15,17] Commercially available porous anodic alumina filters (Whatman Anodisc) were obtained and placed in a 1 in. quartz furnace tube. After heating the tube to temperatures of 700, 750 and 800 °C in flowing argon, ethylene was introduced into the system at a flow rate of 150 sccm. After half an hour in the flowing ethylene ambient, argon was reintroduced into the system and the system was allowed to cool. After this process, the Anodisc membranes were a grayish-black color, due to incorporation of carbon on the surface and interior of the membrane. The samples treated at the highest temperatures almost always curled and became too brittle to handle. We found that

* Corresponding author. E-mail: bcruden@mail.arc.nasa.gov
† Also at Eloret Corporation.

10.1021/nl0350682 CCC: $27.50
Published on Web 12/23/2003

pretreating these samples by clamping them between two alumina plates at the processing temperatures greatly improved their temperature stability and allowed the CVD process to be carried out with yields around 60%.

Representative SEM images of the treated Anodiscs are shown in Figure 1, and the corresponding average diameters and porosities are given in Table 1. After CVD at 700 and 750 °C, the Anodiscs appeared fairly similar to untreated Anodiscs. The only significant difference is a slight expansion of the pore diameter. No carbon overcoating is apparent. The 800 °C treatment, however, showed significant differences. The surface morphology is visually modified, owing to the presence of a carbonaceous film on the surface. A cross-sectional SEM shows that the carbonaceous coating extends down through the pores and is fairly uniform in thickness, conformally covering the surface at a thickness of about 20 nm. The presence of the amorphous carbon film throughout the pores is also confirmed by the fact that the 800 °C sample does not require a metal sputter coating to image. The other samples are nonconductive and charge significantly when subjected to the SEM. It is noteworthy that experimentally measured rates of pyrolytic carbon formation on a glass surface would also predict a film thickness of 20 nm under these conditions.[18] This similarity suggests that growth is not controlled by reactive intermediates, but rather by direct pyrolysis of ethylene on the pore surface. The lower temperature cases would produce films of 3 and 8 nm thicknesses based on the same rate equations. It could be that films near these thicknesses exist in this work but are difficult to detect in the SEM.

The results also indicate that the CVD process is rate-limited by surface reaction pyrolysis rates, and gas transport into the pores is sufficiently well mixed to allow a uniform growth along the length of the pore. This behavior has been observed by others in similar processing.[15] Based on previously measured diffusivity through the pores[1] and the observed growth rates, we can estimate the relative importance of diffusive gas-phase transport to surface reactions, by determining the Thiele modulus, ϕ, as[19]

$$\varphi = \frac{r\rho A_{\text{surf}}}{M}\left(\frac{D}{l}\frac{P}{RT}A_{\text{xsect}}\right)^{-1} \qquad (1)$$

where r is the growth rate, ρ is the density of the carbon film (assumed the same as graphite), M is the molecular weight of carbon, D is the gas-phase diffusivity, P is the gas pressure, R is the ideal gas constant, T is the temperature, l is the pore length, and A_{surf} and A_{xsect} are the surface and cross-sectional areas of a single pore, respectively. Substituting the appropriate numbers, we find a Thiele modulus on the order of 10^{-15}, indicating that gas-phase transport in the pore is very fast relative to the surface reaction rate.

In this work, we have utilized an identical experimental apparatus and theoretical approach to flow characterization as used in our previous work.[1] This work differs from the previous work in that the anodized alumina surfaces have been modified with carbonaceous coatings and the TMAC has been varied in the simulation to capture the behavior induced by this modification. Experimental characterization is performed in a flow tube where pressure drop across the

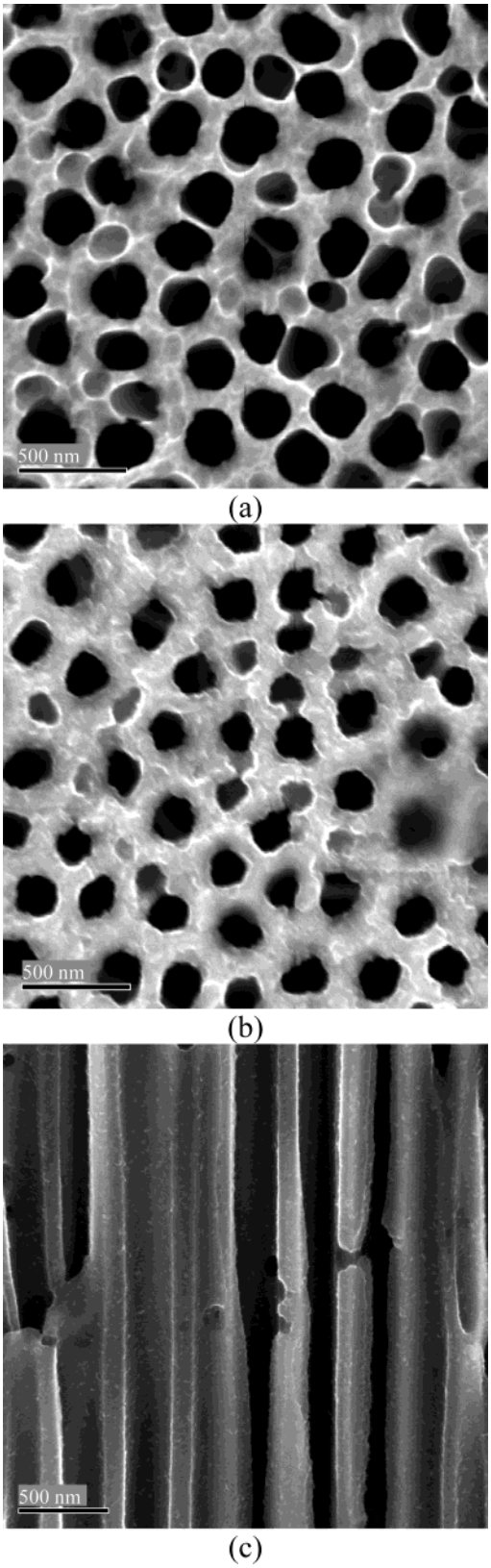

Figure 1. SEM images of Anodisc membrane. (a) Following CVD at 750 °C, looking end on at pore openings. The image is similar to that obtained for an Anodisc without CVD processing. (b) Following CVD at 800 °C. No metal coating was required to obtain the image. (c) Cross-sectional view of the pores in (b).

Table 1. Estimated Properties of the Anodiscs for Varying CVD Processing

CVD temp. (°C)	avg. pore diameter (nm)	avg. pore density ($\times 10^{12}$ m^{-2})	porosity
untreated	212	8.0	0.28
700	235	10.2	0.22
750	220	7.2	0.27
800[a]	169	9.4	0.21

[a] Only the 800 °C sample showed any significant carbon film deposition.

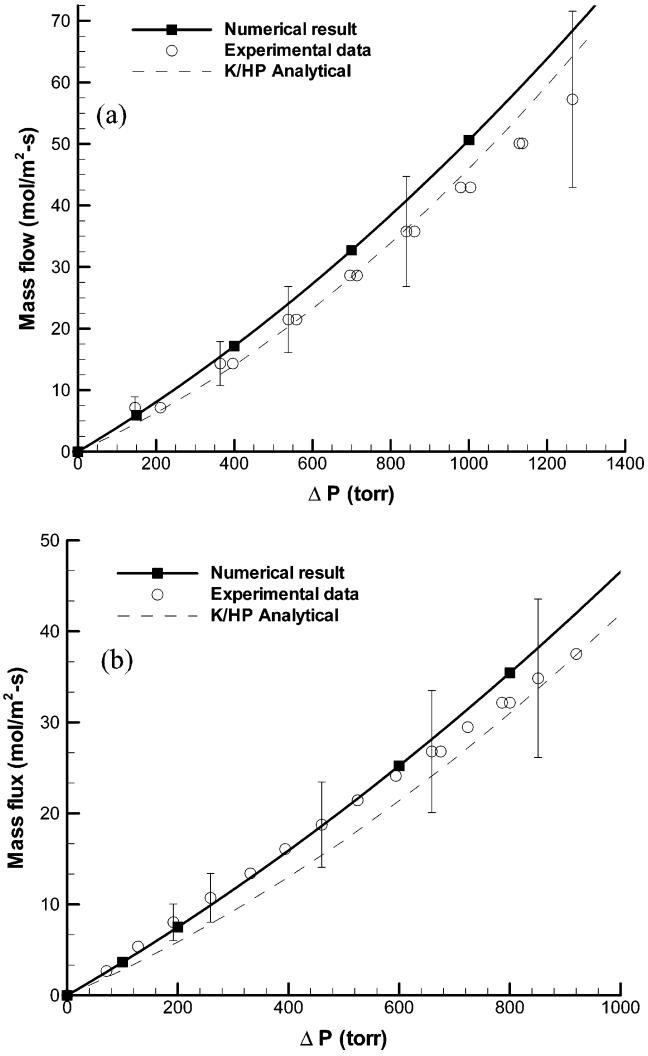

Figure 2. Flux versus pressure drop for argon through Anodisc membranes processed with CVD at temperatures of (a) 700 °C and (b) 750 °C. At these temperatures, the carbon overcoating appears to be negligible. Overlaying the data is the model results with $\sigma_v = 1.0$ and the analytical expression for combined Knudsen/Hagen−Poiseuille transport (K/HP Analytical).

membrane is monitored versus a controlled flow rate. These bulk measurements can be related to the flux through an individual pore by introducing a correction for the membrane porosity. This introduces the largest error into the calculation as the pore areas can vary by as much as 25% across a single sample. This error is a systematic (not random) error so that all data is affected in an identical fashion. Thus, this error would impact a linear fit in the data, but will not impact any curvature present. The relation between flux and pressure

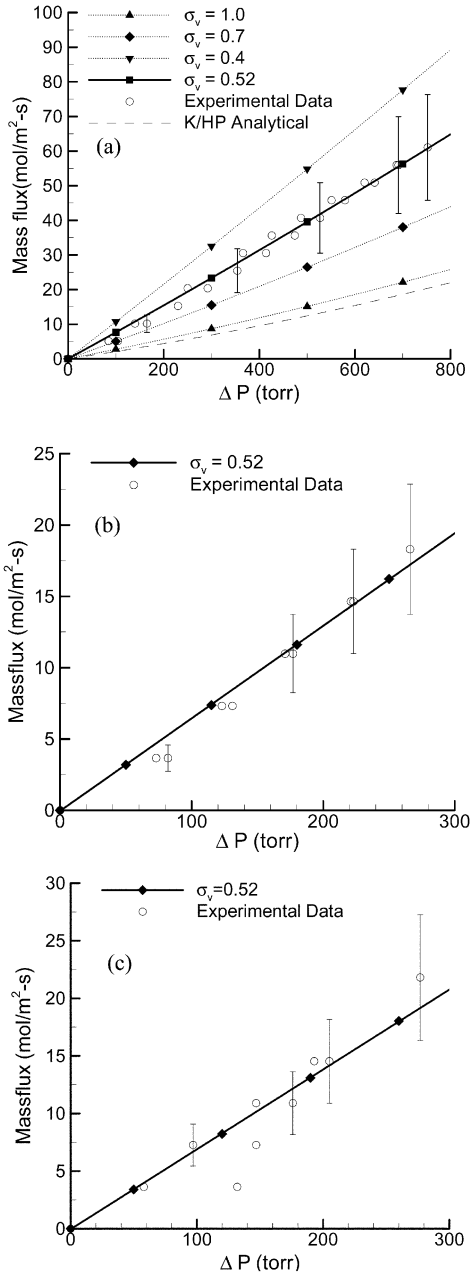

Figure 3. Flux versus pressure drop for Anodisc membranes with a CVD carbon coating deposited at 800 °C. (a) For argon, with model results overlayed for a variety of TMAC values. Also shown is the analytical expression for combined Knudsen diffusion and Hagen−Poiseuille flow. (b) For nitrogen, with the best fit parameter from (a) overlayed on the data. (c) The same for oxygen.

drop is studied for oxygen, nitrogen, and argon. The theoretical approach is a finite element based hydrodynamic model incorporating Navier−Stokes equations with a first-order slip boundary condition. A single adjustable parameter, the TMAC (σ_v), is adjusted to match the behavior observed experimentally for argon. The uncertainty in the data is used to estimate an uncertainty in the derived TMAC. The coefficient obtained for argon is found to match data obtained for oxygen and nitrogen as well.

Figure 2 shows the data obtained for the samples prepared at 700 and 750 °C (i.e., negligible carbon film formation), along with the theoretical analytical solution when transport

is due to a combination of Knudsen diffusion and forced viscous Hagen−Poiseuille flow:

$$J = \frac{2r_p}{3l}\sqrt{\frac{8RT}{\pi M}}\frac{P}{RT} + \frac{\mu r_p^2}{16l}\frac{P^2}{RT} \quad (2)$$

with the first term due to Knudsen diffusion and the second Hagen−Poiseuille flow.[20] Here, M is the molecular weight of the gas, μ is its viscosity, J the flux, and r_p the pore radius. This solution is within the error bounds of the experimental data. However, the error in the data is not random, but rather is a systematic shift that should be the same percentage for all data points. So, while the magnitude is correct, the data lacks the curvature predicted by Hagen−Poiseuille flow. This may be accounted for with a first order slip correction. The hydrodynamic model with slip boundary conditions predicts a relationship between pressure and flux that agrees well with the data when a TMAC of 1.0 is assumed. The percentage difference between model trend and data is approximately constant throughout the range studied, showing that it has predicted the correct curvature, with a magnitude that is within the range of uncertainty. With the inclusion of slip boundary conditions, shear stress induced at the wall is reduced, lessening the impact of viscosity on the flow profile. This reduction in stress at the wall also allows for a larger flux through the pore at identical pressure conditions. These results are nearly identical to the results obtained in our previous work. The major difference stems from a shift in pore diameter.

Figure 3 shows the data obtained on the 800 °C sample, where results differ significantly from combined Knudsen diffusion and Hagen−Poiseuille flow. Comparing the data to the model with a variety of slip coefficients, we find that a slip coefficient of 0.52 gives the best representation of the data obtained for argon. Given the uncertainty in membrane porosity, some error must be assigned to this estimate. As the TMACs of 0.4 and 0.7 are clearly outside of the bounds of uncertainty, based on the numerical prediction a reasonable estimate of $\sigma_v = 0.52 \pm 0.1$ is made. This slip coefficient is then applied to the systems of oxygen and nitrogen, and is found to represent both sets of data well. The lower slip coefficients suggest that the interaction of gas molecules colliding with the coated pore walls tends to reflect in a specular fashion, not losing forward momentum at the wall interface. Consequently, the resistance to flow from wall-induced shear stress is reduced, allowing a greater throughput through the pore at otherwise identical pressures.

It is also possible to obtain an analytical estimate of slip coefficient from the following relations:[21]

$$\frac{\dot{m}}{P_i^2 - P_o^2} = B\frac{1}{\bar{P}} + C$$

$$B = \frac{A_{xsec}\, d^2}{4\mu l RT}\frac{2-\sigma_v}{\sigma_v}Kn_o P_o$$

$$C = \frac{A_{xsec}\, d^2}{24\mu l RT} \quad (3)$$

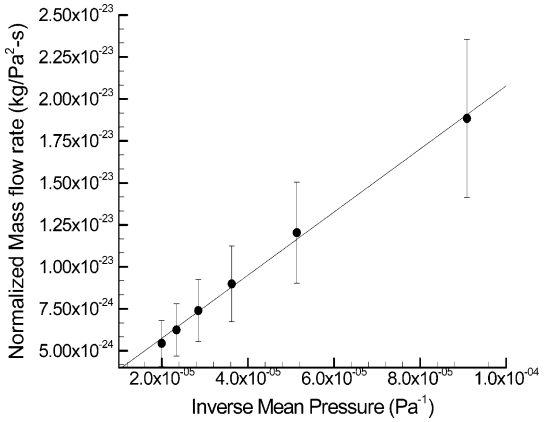

Figure 4. Normalized mass flow rate $\dot{m}/P_i^2 - P_o^2$ for experimental Argon data at 800 °C plotted as a function of the inverse mean pressure $1/\bar{P}$. The slope of the line is utilized to estimate an analytical $\sigma_v = 0.6 \pm 0.1$.

where $\dot{m}$ is the mass flow rate in kg/s, P_i and P_o are the inlet and outlet pressures, $\bar{P} = (P_i + P_o)/2$ is the mean pressure, d is the average pore diameter, and Kn is the Knudsen number. In Figure 4, the normalized mass flow rate experimental argon data from the 800 °C sample is plotted as a function of inverse mean pressure. The slope of this line is then used to estimate the analytical momentum slip coefficient as 0.6 ± 0.1, in close agreement with the slip coefficient derived from the hydrodynamic model.

In conclusion, we have used experimental data and theoretical modeling to estimate the slip coefficient for amorphous carbon nanotubules. This is the first time we are aware of this estimate being made, which may have important consequences to the application of these materials. The hydrodynamic Navier Stokes method with first-order slip condition predicted the experimental results quite well for the range of diameters studied in this paper. Similar apparent success has been reported elsewhere for electroosmotic flow through 5 nm tubes where the continuum model agreed well with molecular dynamics predictions.[22] This shows that the hydrodynamic models for nanoscale flows need to be investigated thoroughly before discarding them. While the diameters of the nanotubules studied here may be too large to make them interesting for gas phase separations, it suggests the possibility of scaling down to smaller tube diameters. Molecular dynamics simulations have suggested that carbon nanotubes, with diameters on the order of a nanometer, will have excellent separation properties due to their size[23] and higher throughputs than similarly sized materials due to their smoothness.[24] While the nanotubules studied here probably do not have the same molecular structure as carbon nanotubes, they do experimentally display a higher throughput due to the carbon coating on their surface. Further experiments need to be performed to determine if this throughput enhancement will apply to carbon nanotubes, though the combination of these results and MD simulations are a favorable suggestion in this direction. Unfortunately, it is experimentally difficult to obtain oriented carbon nanotubes within pores of this nature as the CVD of carbon nanotubes is performed on solid surfaces that are not amenable to end-to-end flow experiments such as performed here.

References

(1) Roy, S.; Raju, R.; Chuang, H. F.; Cruden, B. A.; Meyyappan, M. *J. Appl. Phys.* **2003**, *93*, 4870.
(2) Bird, G. A. *Molecular gas dynamics and the direct simulation of gas flows*; Clarendon Press: New York, 1994.
(3) Karniadakis, G.; Beskok, A. *Micro flows-fundamentals and simulation*. Springer-Verlag: Berlin, 2002.
(4) Burnett, D. *Proc. London Math. Soc.* **1935**, *40*, 382.
(5) Itaya, K.; Sugawara, S.; Arai, K.; Saito, S. *J. Chem. Eng. Jpn.* **1984**, *17*, 514.
(6) Li, F.; Zhang, L.; Metzger, R. K. *Chem. Mater.* **1998**, *10*, 2470.
(7) Masuda, H.; Yamada, H.; Satoh, M.; Asoh, H.; Nakao, M.; Tamamura, T. *Appl. Phys. Lett.* **1997**, *71*, 2770.
(8) Li, J.; Papadopolous, C.; Xu, J. M.; Moskovits, M. *Appl. Phys. Lett.* **1999**, *75*, 367.
(9) Parthasarathy, R. V.; Phani, K. L. N.; Martin, C. R. *Adv. Mater.* **1995**, *7*, 896.
(10) Suh, J. S.; Lee, J. S. *Appl. Phys. Lett.* **1999**, *75*, 2047.
(11) Zhang, X. Y.; Zhang, L. D.; Zheng, M. J.; Li, G. H.; Zhao, L. X. *J. Cryst. Growth* **2001**, *223*, 306.
(12) Tonucci, R. J.; Justus, B. L.; Campillo, A. J.; Ford, C. E. *Science* **1992**, *258*, 783.
(13) Whitney, T. W.; Jiang, J. S.; Searson, P. C.; Chien, C. L. *Science* **1993**, *261*, 1316.
(14) Ichimura, S.; Tsuru, T.; Nakao, S.-I.; Kimura, S. *J. Chem. Eng. Jpn.* **2000**, *33*, 141.
(15) Miller, S. A.; Young, V. Y.; Martin, C. R. *J. Am. Chem. Soc.* **2001**, *123*, 12335.
(16) Che, G.; Lakshmi, B. B.; Martin, C. R.; Fisher, E. R. *Langmuir* **1999**, *15*, 750.
(17) Kyotani, T.; Tsai, L.-f.; Tomita, A. *Chem. Mater.* **1996**, *8*, 2109.
(18) Tesner, P. A. In *Chemistry and physics of carbon: A series of advances*; Thrower, P. A., Ed.; Marcel Dekker: New York, 1984; Vol. 19, p 65.
(19) Fogler, H. S. Prentice Hall: New York, 1999.
(20) Rutherford, S. W.; Do, D. D. *Adsorption* **1997**, *3*, 283.
(21) Arkilic, E. B.; Breuer, K. E.; Schmidt, M. A. *J. Fluid Mech.* **2001**, *437*, 29.
(22) Qiao, R.; Aluru, N. R. *Nanotechnology* **2002**, *1*, 28.
(23) Mao, Z.; Sinnott, S. B. *J. Phys. Chem. B* **2001**, *105*, 6916.
(24) Skoulidas, A. I.; Ackerman, D. M.; Johnson, J. K.; Sholl, D. S. *Phys. Rev. Lett.* 2002, 89.

NL0350682